Benchmarking Atomistic Simulations against the ThermoML Data Archive: Neat Liquid Densities and Static Dielectric Constants

Kyle A. Beauchamp[+],[1,*] Julie M. Behr[+],[2,†] Patrick B. Grinaway,[3,‡]
Arien S. Rustenburg,[3,§] Kenneth Kroenlein,[4,¶] and John D. Chodera[1,**]

[1]*Computational Biology Program, Sloan Kettering Institute, Memorial Sloan Kettering Cancer Center, New York, NY*
[2]*Tri-Institutional Program in Computational Biology and Medicine, Weill Cornell Medical College, New York, NY*
[3]*Graduate Program in Physiology, Biophysics, and Systems Biology, Weill Cornell Medical College, New York, NY*
[4]*Themodynamics Research Center, NIST, Boulder, CO*

(Dated: March 11, 2015)

Useful atomistic simulations in the condensed phase require accurate depictions of solvent. While experimental measurements of fundamental physical properties offer a straightforward approach for evaluating forcefield quality, the bulk of this information has been tied up in formats that are not machine-readable. These formats require substantial human effort to compile benchmark datasets which are prone to accumulation of human errors, hindering the development of reproducible benchmarks of forcefield accuracy. Here, we examine the feasibility of benchmarking atomistic forcefields against the NIST ThermoML data archive of physicochemical measurements, which aggregates thousands of experimental measurements in a portable, machine-readable, self-annotating format. As a proof of concept, we present a detailed benchmark of the generalized Amber small molecule forcefield (GAFF) using the AM1-BCC charge model against measurements (specifically liquid densities and static dielectric constants at ambient pressure) automatically extracted from the archive, and discuss the extent of available data for neat liquids. The results of this benchmark highlights a general problem with fixed-charge forcefields in the representation of liquids of low dielectric.

Keywords: molecular mechanics forcefields; forcefield parameterization; forcefield accuracy; forcefield validation; mass density; static dielectric constant

I. INTRODUCTION

Recent advances in hardware and software for molecular dynamics simulation now permits routine access to atomistic simulations at the 100 ns timescale and beyond [1]. Leveraging these advances in combination with consumer GPU clusters, distributed computing, or custom hardware has brought microsecond and millisecond simulation timescales within reach of many laboratories. These dramatic advances in sampling, however, have revealed deficiencies in forcefields as a critical barrier to enabling truly predictive simulations of physical properties of biomolecular systems.

Protein and water forcefields have been the subject of numerous benchmarks [2] and enhancements [3–5], with key outcomes including the ability to fold fast-folding proteins [6–8], improved fidelity of water thermodynamic properties [9], and improved prediction of NMR observables. Although small molecule forcefields have also been the subject of benchmarks [10] and improvements [11], such work has typically focused on small perturbations to specific functional groups. For example, a recent study found that modified hydroxyl nonbonded parameters led to improved prediction of static dielectric constants and hydration free energies [11]. There are also outstanding questions of generalizability of these targeted perturbations; it is uncertain whether changes to the parameters for a specific chemical moiety will be compatible with seemingly unrelated improvements to other groups. Addressing these questions requires establishing a community agreement on shared benchmarks that can be easily replicated among laboratories to test proposed forcefield enhancements and expanded as the body of experimental data grows.

A key barrier to establishing reproducible and extensible forcefield accuracy benchmarks is that many experimental datasets are heterogeneous, paywalled, and unavailable in machine-readable formats (although notable counterexamples exist, e.g. the RCSB [12], FreeSolv [13], and the BMRB [14]). While this inconvenience is relatively minor for benchmarking forcefield accuracy for a single target (e.g. water), it becomes prohibitive for studies spanning the relevant chemical space. To ameliorate problems of data archival, the NIST Thermodynamics Research Center (TRC) has developed a IUPAC standard XML-based format—ThermoML [15]—for storing physicochemical measurements, uncertainties, and metadata. Experimental researchers publishing measurements in several journals (J. Chem. Eng. Data, J. Chem. Therm., Fluid Phase Equil., Therm. Acta, and Int. J. Therm.) are guided through a data archival process that involves sanity checks, conversion to a standard machine-readable format, and archival at the TRC (`http://trc.nist.gov/ThermoML.html`).

* kyle.beauchamp@choderalab.org
† julie.behr@choderalab.org
‡ patrick.grinaway@choderalab.org
§ bas.rustenburg@choderalab.org
¶ kenneth.kroenlein@nist.gov
** Corresponding author; john.chodera@choderalab.org

Here, we examine the ThermoML archive as a potential source for providing the foundation for a reproducible, extensible accuracy benchmark of biomolecular forcefields. In particular, we concentrate on two important physical property measurements easily computable in many simulation codes—neat liquid density and static dielectric constant measurements—with the goal of developing a standard benchmark for validating these properties in fixed-charge forcefields of drug-like molecules and biopolymer residue analogues. These two properties provide sensitive tests of forcefield accuracy that are nonetheless straightforward to calculate. Using these data, we evaluate the generalized Amber small molecule forcefield (GAFF) [16] with the AM1-BCC charge model [17, 18] and identify systematic biases to aid further forcefield refinement.

II. METHODS

A. ThermoML Processing

A tarball archive of the ThermoML Archive was obtained from the the NIST TRC on 13 Sep 2014. To explore the content of this archive, we created a Python (version 2.7.9) tool (ThermoPyL: https://github.com/choderalab/ThermoPyL) that formats the XML content into a spreadsheet-like format accessible via the Pandas (version 0.15.2) library. First, we obtained the XML schema (http://media.iupac.org/namespaces/ThermoML/ThermoML.xsd) defining the layout of the data. This schema was converted into a Python object via PyXB 1.2.4 (http://pyxb.sourceforge.net/). Finally, this schema and Pandas was used to extract the data and apply the successive data filters described in Section III A.

B. Simulation

Using an automated tool, boxes of 1000 molecules were constructed using PackMol version 14-225 [19]. AM1-BCC [17, 18] charges were generated using OpenEye Toolkit 2014-6-6 [20], using the `oequacpac.OEAssignPartialCharges` module with the `OECharges_AM1BCCSym` option, which utilizes a conformational expansion procedure prior to charge fitting to minimize artifacts from intramolecular contacts. The selected conformer was then processed using antechamber in AmberTools 14 [21]. The resulting AMBER files were converted to OpenMM [22] ffxml forcefield XML files. Simulation code used libraries gaff2xml 0.6, TrustButVerify 0.1, OpenMM 6.2 [22], and MDTraj 1.3 [23]. [TODO: Provide a script to install all of these versions via `conda`.]

Molecular dynamics simulations were performed with OpenMM 6.2 [22] using a Langevin integrator (with collision rate 1 ps^{-1}) and a 1 fs timestep, as we found that timesteps of 2 fs timestep or greater led to a significant timestep dependence in computed equilibrium densities (Table 4). [JDC: Cite Langevin integrator used in OpenMM.] Pressure control to 1 atm was achieved with a Monte Carlo barostat utilizing molecular scaling and automated step size adjustment during equilibration, with volume moves attempted every 25 steps. The particle mesh Ewald (PME) method [24] was used with a long-range cutoff of 0.95 nm and a long-range isotropic dispersion correction. [JDC: Can we report the automatically-selected PME parameters to aid reproducibility in other codes?] Simulations were continued until density standard errors were less than 2×10^{-4} g / mL, as estimated using the equilibration detection module in pymbar 2.1 [25]. Trajectory analysis was performed using OpenMM 6.2 [22] and MDTraj 1.3 [23]. Instantaneous densities were stored every 250 fs, while trajectory snapshots were stored every 10 ps. [JDC: Did we plan to make this data available somewhere, or is it sufficient to put out the scripts?] Static dielectric constants were calculated using the dipole fluctuation approach [9], with box dipoles calculated from trajectory files using MDTraj 1.3 [23].

$$\epsilon = 1 + \frac{4\pi}{3} \frac{\langle \mu \cdot \mu \rangle - \langle \mu \rangle \cdot \langle \mu \rangle}{\langle V \rangle k_B T} \tag{1}$$

III. RESULTS

A. Extracting neat liquid measurements from the NIST TRC ThermoML Archive

We retrieved a copy of the ThermoML Archive from the NIST TRC (http://trc.nist.gov/ThermoML.html accessed 13 Sep 2014) and performed a number of sequential filtering steps to produce an extract of the ThermoML Archive relevant for benchmarking forcefields describing small organic molecules. As our aim is to explore neat liquid data with functional groups relevant to biopolymers and drug-like molecules, we applied the following ordered filters, starting with all data containing density or static dielectric constants:

1. The measured solution contains only a single component (e.g. no binary mixtures)
2. The molecule contains only the druglike elements (defined here as H, N, C, O, S, P, F, Cl, Br)
3. The molecule has ≤ 10 heavy atoms
4. The measurement was performed in a biophysically relevant temperature range [K] $(270 \leq T \leq 330)$
5. The measurement was performed at ambient pressure [kPA] $(100 \leq P \leq 102)$
6. Measured densities below 300 kg m^{-3} were discarded to eliminate gas-phase measurements
7. The temperature and pressure were rounded to nearby values (as described below), averaging all measurements within each group of like conditions

Filter step	Number of measurements remaining: Mass density	Static dielectric
1. single component	130074	1649
2. only druglike elements	120410	1649
3. $\leq$10 heavy atoms	67897	1567
4. $(270 \leq T \leq 330)$ [K]	36827	962
5. ambient pressure	13598	461
6. liquid state	13573	461
7. aggregate T, P	3573	432
8. density and dielectric	245	245

TABLE I. Successive filtration of the ThermoML Archive. A set of successive filters were applied to all measurements in the ThermoML Archive (accessed 13 Sep 2014) that contained either mass density or static dielectric constant measurements. Each column reports the number of measurements remaining after successive application of the corresponding filtration step.

8. Only conditions (molecule, temperature, pressure) for which *both* density and dielectric constants were available were retained

The temperature and pressure rounding step was motivated by common data reporting variations; for example, an experiment performed at water's freezing point at ambient pressure might be entered as either 101.325 kPA or 100 kPA, with a temperature of either 273 K or 273.15 K. Therefore all pressures within the range [kPA] $(100 \leq P \leq 102)$ were rounded to exactly one atmosphere. Temperatures were rounded to one decimal place. The application of these filters (Table I) leaves 245 conditions—where a *condition* here indicates a (molecule, temperature, pressure) tuple—for which both density and dielectric data are available. The functional groups present in the resulting dataset are summarized in Table II; see Methods for further description of the software pipeline used.

B. Benchmarking GAFF/AM1-BCC against the ThermoML Archive

1. Mass density

Mass density has been widely used for parameterizing and testing forcefields, particularly the Lennard-Jones parameters representing dispersive and repulsive interactions [27, 28]. We therefore used the present ThermoML extract as a benchmark of the GAFF/AM1-BCC forcefield (Fig. 1). We estimate the mass density via $\rho = \langle \frac{M}{V} \rangle$.

Overall, the densities show reasonable accuracy, with a root-mean square (RMS) relative error over all measurements of 2.8$\pm$0.1% (with one standard error of the mean determined by bootstrapping over all measurements), especially encouraging given that this forcefield was not designed with the intention of modeling bulk liquid properties of organic molecules [16] This is reasonably consistent with previous studies reporting agreement of 4% on a different benchmark set [10].

[JDC: Discuss outliers here. There must be more things we can say about densities. Some of the densities are quite good, while others seem poor, with systematic bias toward higher densities than experiment. We can also point out that densities at different temperatures for a given molecule seem to be biased in a consistent way.]

Functional Group	Occurrences
1,2-aminoalcohol	4
1,2-diol	3
alkene	3
aromatic compound	1
carbonic acid diester	2
carboxylic acid ester	4
dialkyl ether	7
heterocyclic compound	3
ketone	2
lactone	1
primary alcohol	19
primary aliphatic amine (alkylamine)	2
primary amine	2
secondary alcohol	4
secondary aliphatic amine (dialkylamine)	2
secondary aliphatic/aromatic amine (alkylarylamine)	1
secondary amine	3
sulfone	1
sulfoxide	1
tertiary aliphatic amine (trialkylamine)	3
tertiary amine	3

TABLE II. Functional groups present in filtered dataset. The filtered ThermoML dataset contained 245 distinct (molecule, temperature, pressure) conditions, spanning 44 unique compounds. The functional groups represented in these compounds (as identified by the program `checkmol` v0.5 [26]) is summarized here.

2. Static dielectric constant

As a measure of the dielectric response, the static dielectric constant of neat liquids provides a critical benchmark of the accuracy electrostatic treatment in forcefield models. We therefore compare simulations against the measurements in our ThermoML extract. Overall, we find the dielectric constants to be qualitatively reasonable, but with clear deviations from experiment. In particular, GAFF/AM1-BCC systematically underestimates the dielectric constants for nonpolar organics, with the predictions of $\epsilon \approx 1.0 \pm 0.05$ being substantially smaller than the measured $\epsilon \approx 2$. Because this deviation likely stems from the lack of an explicit treatment of electronic polarization, we used a simple empirical polarization model that computes the molecular electronic polarizability α a sum of elemental atomic polarizability contributions [29]. From the computed molecular electronic polarizability α, an additive correction to the simulation-derived static dielectric constant accounting for the missing electronic polarizability can be computed [9]

$$\Delta\epsilon = 4\pi N \frac{\alpha}{\langle V \rangle} \quad (2)$$

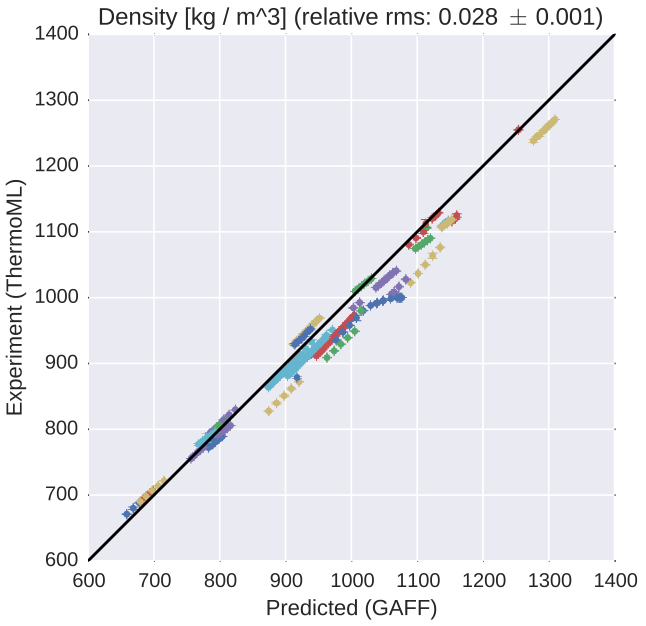

FIG. 1. Comparison of liquid densities between experiment and simulation. Liquid density measurements extracted from ThermoML are compared against densities predicted using the GAFF/AM1-BCC small molecule fixed-charge forcefield. Color groupings represent identical chemical species. Simulation error bars represent one standard error of the mean, with the number of effective (uncorrelated) samples estimated using pymbar. Experimental error bars indicate the standard deviation between independently reported measurements, when available, or author-reported standard deviations in ThermoML entries; for some measurements, neither uncertainty estimate is available. See SI Fig. 5 for further discussion of error.

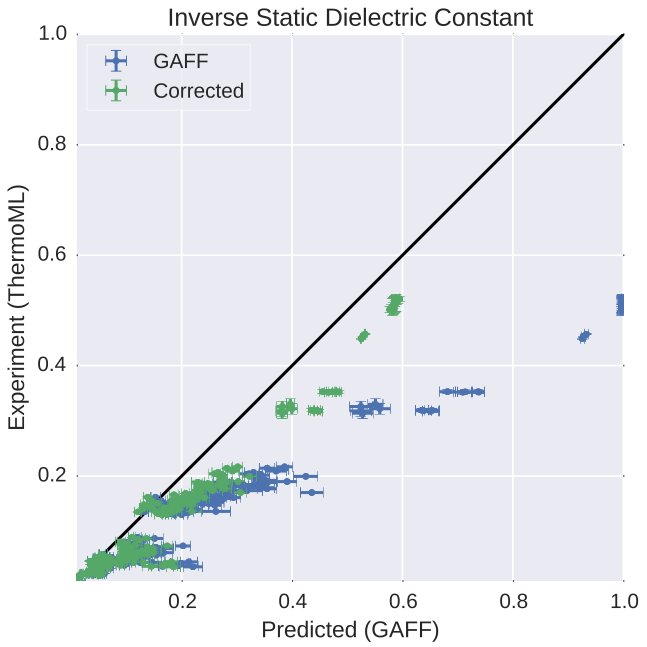

FIG. 2. Measured (ThermoML) versus predicted (GAFF/AM1-BCC) inverse static dielectrics (a). Simulation error bars represent one standard error of the mean estimated via circular block averaging [30] with block sizes automatically selected to maximize the error [31]. Experimental error bars indicate the larger of standard deviation between independently reported measurements and the authors reported standard deviations; for some measurements, neither uncertainty estimate is available. See SI Fig. 5 for further discussion of error. The inverse dielectric constant ϵ^{-1} is plotted instead of ϵ because ϵ^{-1} is directly proportional to the Coulomb interaction energy between point charges embedded in a dielectric material [e.g. $U(r) \propto q_1 q_2 / r \propto \epsilon^{-1}$].

While a similar polarization correction was used in the development of the TIP4P-Ew water model, where it had a minor effect [9], missing polarizability is a dominant contribution to the static dielectric constant of nonpolar organic molecules; in the case of water, the empirical atomic polarizability model predicts a dielectric correction of 0.52, while 0.79 was used for the TIP4P-Ew model. Considering all predictions in the present work leads to polarizability corrections to the static dielectric of 0.74 ± 0.08.

IV. DISCUSSION

A. Fitting Forcefields to Dielectric Constants

Recent forcefield development has seen a resurgence of papers fitting dielectric constants during forcefield parameterization [11, 32]. However, a number of authors have pointed out potential challenges in constructing self-consistent fixed-charge forcefields [33, 34].

Interestingly, recent work by Dill and coworkers [33] observed that, for CCl_4, reasonable choices of point charges are incapable of recapitulating the observed dielectric of $\epsilon = 2.2$, instead producing dielectric constants in the range of $1.0 \leq \epsilon \leq 1.05$. This behavior is quite general: fixed point charge forcefields will predict $\epsilon \approx 1$ for many nonpolar or symmetric molecules, but the measured dielectric constants are instead $\epsilon \approx 2$ (Fig. 3). While this behavior is well-known and results from missing physics of polarizability, we suspect it may have several unanticipated consequences, which we discuss below.

Suppose, for example, that one attempts to fit forcefield parameters to match the static dielectric constants of CCl_4, $CHCl_3$, CH_2Cl_2, and CH_3Cl. In moving from the tetrahedrally-symmetric CCl_4 to the asymmetric $CHCl_3$, it suddenly becomes possible to achieve the observed dielectric constant of 4.8 by an appropriate choice of point charges. However, the model for $CHCl_3$ uses fixed point charges to account for *both* the permanent dipole moment and the electronic polarizability, whereas the CCl_4 model contains no treatment of polarizability. We hypothesize that this inconsistency in parameterization may lead to strange mismatches, where symmetric molecules (e.g. benzene and CCl_4) have qualitatively different properties than closely related asymmetric molecules (e.g. toluene and $CHCl_3$).

How important is this effect? As a possible real-world example, we imagine that the missing atomic polarizabil-

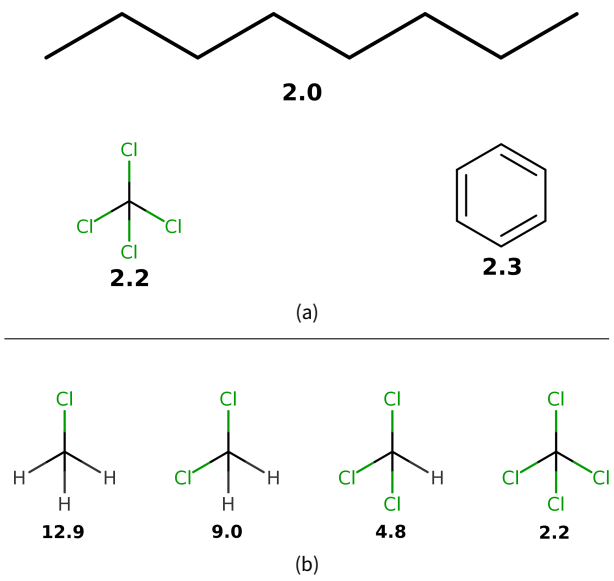

FIG. 3. Typical experimental static dielectric constants of some nonpolar compounds. (a). Measured static dielectric constants of various nonpolar or symmetric molecules [35, 36]. Fixed-charge forcefields give $\epsilon \approx 1$ for each species; for example, we calculated $\epsilon = 1.003 \pm 0.0002$ for octane. (b). A congeneric series of chloro-substituted methanes have static dielectric constants between 2 and 13. Reported dielectric constants are at near-ambient temperatures.

ity could be important in accurate transfer free energies involving low-dielectric solvents. The Onsager model for the transfer free energy of a dipole (Eq. 3) gives an error of $\Delta\Delta G = \Delta G(\epsilon = 2.2) - \Delta G(\epsilon = 1)$ of -2 kcal / mol for the transfer of water ($a = 1.93$ Å, $\mu = 2.2$D) into a low dielectric medium such as tetrachloromethane or benzene.

$$\Delta G = -\frac{\mu^2}{a^3}\frac{\epsilon - 1}{2\epsilon + 1} \tag{3}$$

$$\Delta\Delta G = -\frac{\mu^2}{a^3}\left[\frac{\epsilon_1 - 1}{2\epsilon_1 + 1} - \frac{\epsilon_2 - 1}{2\epsilon_2 + 1}\right] \tag{4}$$

Similarly, we calculated the mean polarization error for solvation free energies (gas to solvent transfer free energies) of druglike molecules in cyclohexane. For each molecule in the latest (Feb. 20) FreeSolv database [13, 37], we took the cavity radius a to be the half the maximum interatomic distance and calculated $\mu = \sum_i q_i r_i$ using the provided mol2 coordinates and AM1-BCC charges. This calculation predicts a mean error of -0.91 ± 0.07 kcal / mol for the 643 molecules (where the standard error is computed from bootstrapping over measurements), suggesting that the missing atomic polarizabilty unrepresentable by fixed point charge forcefields could contribute substantially to errors in predicted transfer and solvation properties of druglike molecules. We also conjecture that

Given their ease of measurement and direct connection to long-range electrostatic interactions, static dielectric constants have high potential utility as primary data for forcefield parameterization efforts. Although this will require the use of forcefields with explicit treatment of atomic polarizability, the inconsistency of fixed-charge models in low-dielectric media is sufficiently alarming to motivate further study of polarizable forcefields. In particular, continuum methods [38–40], point dipole methods [41, 42], and Drude methods [43, 44] have been maturing rapidly. Finding the optimal balance of accuracy and performance remains an open question; however, the use of experimentally-parameterized direct polarization methods [45] may provide polarizability physics at a cost not much greater than fixed charge forcefields.

B. ThermoML as a data source

The present work has focused on the neat liquid density and dielectric measurements present in the ThermoML Archive [15, 46, 47] as a target for molecular dynamics forcefield validation. While liquid mass densities and static dielectric constants have already been widely used in forcefield work, several aspects of ThermoML make it a unique resource for the forcefield community. First, the aggregation, support, and dissemination of ThermoML datasets through the ThermoML Archive is supported by NIST, whose mission makes these tasks a long-term priority. Second, the ThermoML Archive is actively growing, through partnerships with several journals, and new experimental measurements published in these journals are critically examined by the TRC and included in the archive. [JDC: Is the number of journal here also expanding?] Finally, the files in the ThermoML Archive are portable and machine readable via a formal XML schema, allowing facile access to hundreds of thousands of measurements. Numerous additional physical properties contained in ThermoML—including activity coefficients, diffusion constants, boiling point temperatures, critical pressures and densities, coefficients of expansion, speed of sound measurements, viscosities, excess molar enthalpies, heat capacities, and volumes—for neat phases and mixtures represent a rich dataset of high utility for forcefield validation and parameterization.

V. CONCLUSIONS

- ThermoML is a potentially useful resource for the forcefield community
- We have curated a subset of the ThermoML Data Archive for neat liquids with druglike atoms, with thousands of densities and hundreds of dielectrics
- Empirical polarization models correct a systematic bias in comparing fixed-charge forcefields to static dielectric constants

VI. ACKNOWLEDGEMENTS

We thank Vijay S. Pande (Stanford University), Lee-Ping Wang (Stanford University), Peter Eastman (Stanford University), Robert McGibbon (Stanford University), Jason Swails (Rutgers University), David L. Mobley (University of California, Irvine), Christopher I. Bayly (OpenEye Software), Michael R. Shirts (University of Virginia), and members of Chodera lab for helpful discussions. Support for JMB was provided by the Tri-Institutional Training Program in Computational Biology and Medicine (via NIH training grant 1T32GM083937). [JDC: Need support acknowledgments for Patrick and Bas.]

VII. DISCLAIMERS

This contribution of the National Institute of Standards and Technology (NIST) is not subject to copyright in the United States. Products or companies named here are cited only in the interest of complete technical description, and neither constitute nor imply endorsement by NIST or by the U.S. government. Other products may be found to serve as well.

Appendix A: Supplementary Information

All information below this point will eventually be pulled into a separate SI. This will happen closer to submission, as the formatting may be journal-specific. The references may be split in two as well, depending on journal. [JDC: It may be fine to leave this as an Appendix.]

- Figure: Timestep-dependence of density
- Figure: Error analysis for ThermoML dataset
- Table (CSV File): ThermoML Dataset used in present analysis.

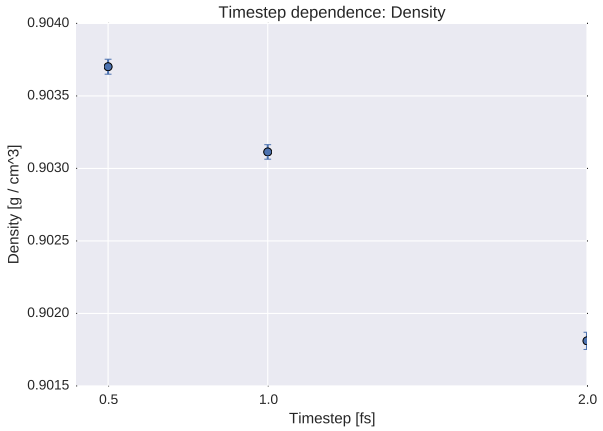

(a)

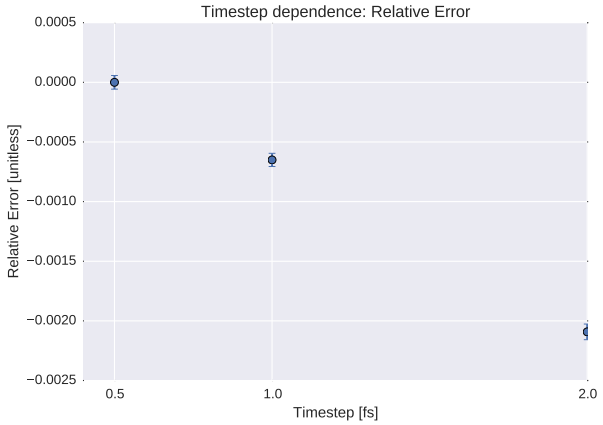

(b)

FIG. 4. To probe the systematic error from finite time-step integration, we examined the timestep dependence of butyl acrylate density. (a). The density is shown for several choices of timestep. (b). The relative error, as compared to the 0.5 fs value, is shown for several choices of timestep. Error bars represent stand errors of the mean, with the number of effective samples estimated using pymbar's statistical inefficiency routine [25]. We find a 2 fs timestep leads to systematic biases in the density on the order of 0.2%, while 1 fs reduces the systematic bias to less than 0.1%—we therefore selected a 1 fs timestep for the present work, where we aimed to achieve three digits of accuracy in density predictions.

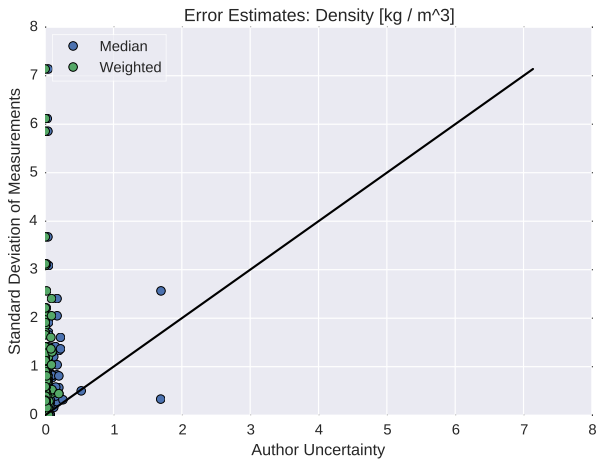

(a)

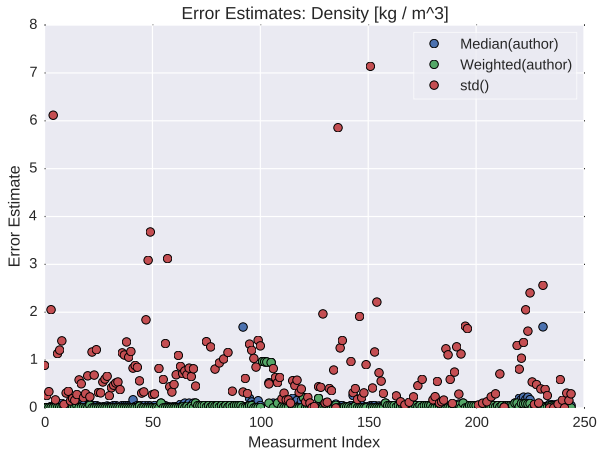

(b)

FIG. 5. **Assessment of experimental error: Density** To assess the experimental error in our ThermoML extract, we compared three difference estimates of uncertainty. In the first approach (Weighted), we computed the standard deviation of the optimally weighted average of the measurements, using the uncertainties reported by authors ($\sigma_{Weighted} = [\sum_k \sigma_k^{-2}]^{-0.5}$). This uncertainty estimator places the highest weights on measurements with small uncertainties and is therefore easily dominated by small outliers and uncertainty under-reporting. In the second approach (Median), we estimated the median of the uncertainties reported by authors; this statistic should be robust to small and large outliers of author-reported uncertainties. In the third approach (Std), we calculated at the standard deviation of independent measurements reported in the ThermoML extract, completely avoiding the author-reported uncertainties. Plot (a) compares the three uncertainty estimates. We see that author-reported uncertainties appear to be substantially smaller than the scatter between the observed measurements. A simple psychological explanation might be that because density measurements are more routine, the authors simply report the accuracy limit of their hardware (e.g. 0.0001 g / mL for a Mettler Toledo DM40 [48]). However, this hardware limit is not achieved due to inconsistencies in sample preparation; see Appendix in Ref. [49]. Panel (b) shows the same information as (a) but as a function of the measurement index, rather than as a scatter plot—because not all measurements have author-supplied uncertainties, panel (c) contains slightly more data points than (a, b).

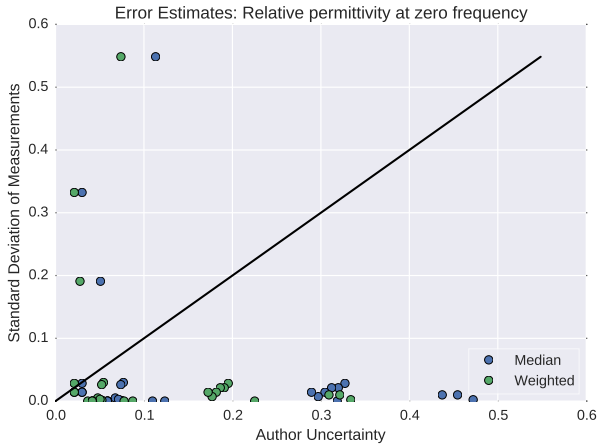

(a)

(b)

FIG. 6. **Assessment of experimental error: Static Dielectric Constant** To assess the experimental error in our ThermoML extract, we compared three difference estimates of uncertainty. In the first approach (Weighted), we computed the standard deviation of the optimally weighted average of the measurements, using the uncertainties reported by authors ($\sigma_{Weighted} = [\sum_k \sigma_k^{-2}]^{-0.5}$). This uncertainty estimator places the highest weights on measurements with small uncertainties and is therefore easily dominated by small outliers and uncertainty under-reporting. In the second approach (Median), we estimated the median of the uncertainties reported by authors; this statistic should be robust to small and large outliers of author-reported uncertainties. In the third approach (Std), we calculated at the standard deviation of independent measurements reported in the ThermoML extract, completely avoiding the author-reported uncertainties. Plot (a) compares the three uncertainty estimates. Unlike the case of densities, author-reported uncertainties appear to be somewhat larger than the scatter between the observed measurements. Panel (b) shows the same information as (a) but as a function of the measurement index, rather than as a scatter plot—because not all measurements have author-supplied uncertainties, panel (c) contains slightly more data points than (a, b).

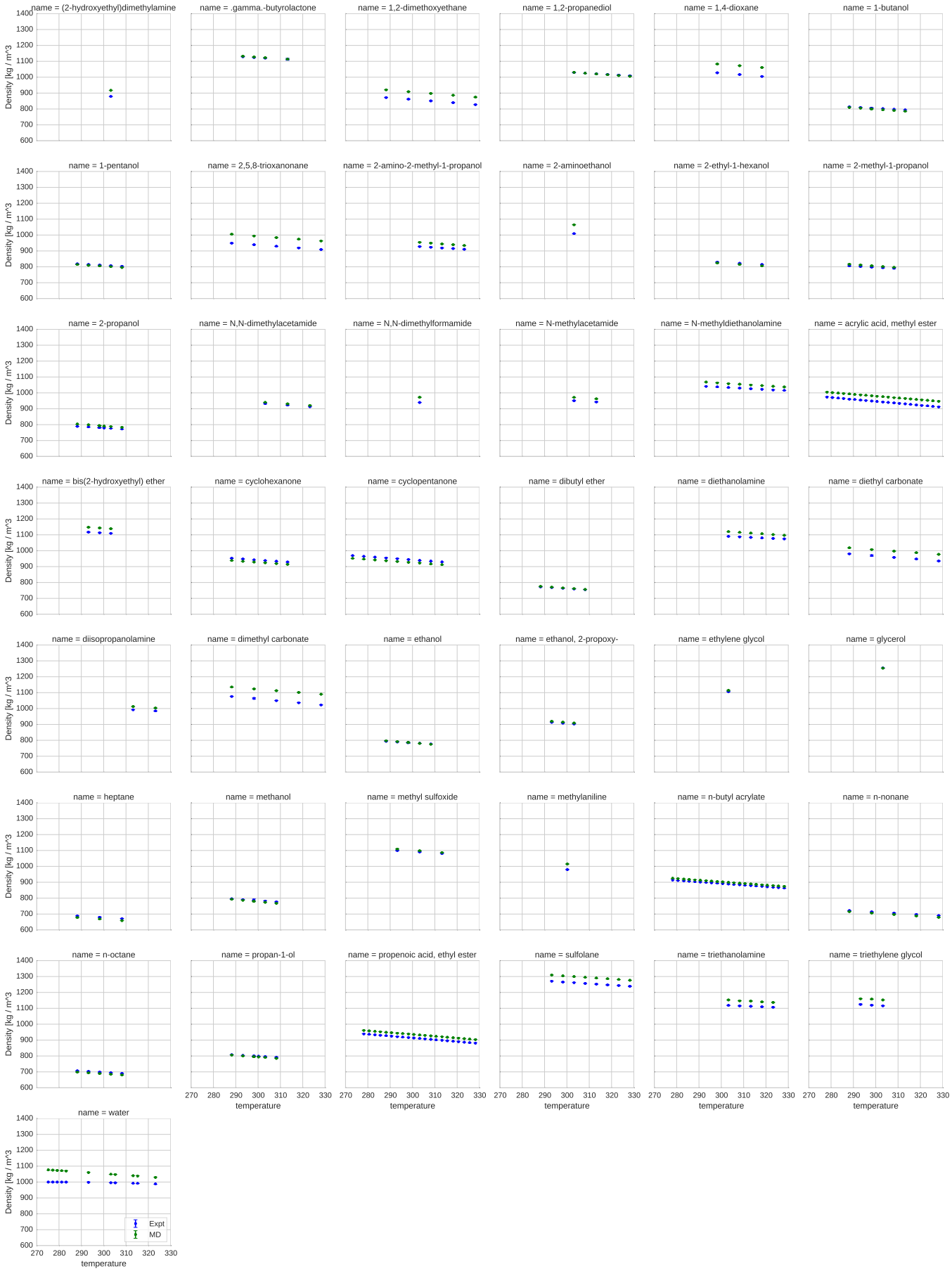

FIG. 7. **Comparison of simulated and experimental densities for all compounds.** Measured (blue) and simulated (green) densities are shown in units of kg/m^3.

FIG. 8. **Comparison of simulated and experimental static dielectric constants for all compounds.** Measured (blue), simulated (green), and polarizability-corrected simulated (red) static dielectric constants are shown for all compounds. Note that dielectric constants, rather than inverse dielectric constants, are plotted here. [JDC: Let's plot these as in Fig. 1 and Fig. 2, maybe only four plots across so they are larger and more legible. We can also shorten "name = compound" to just "compound".] KAB: We should discuss this more before I rebuild this figure several times.

[1] R. Salomon-Ferrer, A. W. GoÌĹtz, D. Poole, S. Le Grand, and R. C. Walker, Journal of Chemical Theory and Computation **9**, 3878 (2013).

[2] K. Lindorff-Larsen, P. Maragakis, S. Piana, M. Eastwood, R. Dror, and D. Shaw, PloS one **7**, e32131 (2012).

[3] D.-W. Li and R. Bruschweiler, J. Chem. Theory Comput. **7**, 1773 (2011).

[4] R. B. Best, X. Zhu, J. Shim, P. E. Lopes, J. Mittal, M. Feig, and A. D. MacKerell, J. Chem. Theory Comput. (2012).

[5] K. Lindorff-Larsen, S. Piana, K. Palmo, P. Maragakis, J. Klepeis, R. Dror, and D. Shaw, Proteins: Struct., Funct., Bioinf. **78**, 1950 (2010).

[6] K. Lindorff-Larsen, S. Piana, R. Dror, and D. Shaw, Science **334**, 517 (2011).

[7] D. Ensign, P. Kasson, and V. Pande, J. Mol. Biol. **374**, 806 (2007).

[8] V. Voelz, G. Bowman, K. Beauchamp, and V. Pande, J. Am. Chem. Soc. **132**, 1526 (2010).

[9] H. Horn, W. Swope, J. Pitera, J. Madura, T. Dick, G. Hura, and T. Head-Gordon, J. Chem. Phys. **120**, 9665 (2004).

[10] C. Caleman, P. J. van Maaren, M. Hong, J. S. Hub, L. T. Costa, and D. van der Spoel, Journal of chemical theory and computation **8**, 61 (2011).

[11] C. J. Fennell, K. L. Wymer, and D. L. Mobley, The Journal of Physical Chemistry B (2014).

[12] H. M. Berman, J. Westbrook, Z. Feng, G. Gilliland, T. N. Bhat, H. Weissig, I. N. Shindyalov, and P. E. Bourne, Nucleic Acids Res. **28**, 235 (2000).

[13] D. L. Mobley, *Experimental and calculated small molecule hydration free energies*, Retrieved from: http://www.escholarship.org/uc/item/6sd403pz, uC Irvine: Department of Pharmaceutical Sciences, UCI.

[14] E. Ulrich, H. Akutsu, J. Doreleijers, Y. Harano, Y. Ioannidis, J. Lin, M. Livny, S. Mading, D. Maziuk, and Z. Miller, Nucleic Acids Res. **36**, D402 (2008).

[15] M. Frenkel, R. D. Chiroco, V. Diky, Q. Dong, K. N. Marsh, J. H. Dymond, W. A. Wakeham, S. E. Stein, E. Königsberger, and A. R. Goodwin, Pure and applied chemistry **78**, 541 (2006).

[16] J. Wang, R. M. Wolf, J. W. Caldwell, P. A. Kollman, and D. A. Case, J. Comput. Chem. **25**, 1157 (2004).

[17] A. Jakalian, B. L. Bush, D. B. Jack, and C. I. Bayly, J. Comput. Chem. **21**, 132 (2000).

[18] A. Jakalian, D. B. Jack, and C. I. Bayly, J. Comput. Chem. **23**, 1623 (2002).

[19] L. Martínez, R. Andrade, E. G. Birgin, and J. M. Martínez, Journal of computational chemistry **30**, 2157 (2009).

[20] *Openeye toolkits 2014*, URL http://www.eyesopen.com.

[21] D. Case, V. Babin, J. Berryman, R. Betz, Q. Cai, D. Cerutti, T. Cheatham III, T. Darden, R. Duke, H. Gohlke, et al., University of California, San Francisco (2014).

[22] P. Eastman, M. S. Friedrichs, J. D. Chodera, R. J. Radmer, C. M. Bruns, J. P. Ku, K. A. Beauchamp, T. J. Lane, L.-P. Wang, D. Shukla, et al., J. Chem. Theory Comput. **9**, 461 (2012).

[23] R. T. McGibbon, K. A. Beauchamp, C. R. Schwantes, L.-P. Wang, C. X. Hernández, M. P. Harrigan, T. J. Lane, J. M. Swails, and V. S. Pande, bioRxiv p. 008896 (2014).

[24] T. Darden, D. York, and L. Pedersen, J. Chem. Phys. **98**, 10089 (1993).

[25] M. R. Shirts and J. D. Chodera, J. Chem. Phys. **129**, 124105 (2008).

[26] N. Haider, Molecules **15**, 5079 (2010).

[27] W. L. Jorgensen, J. Chandrasekhar, J. D. Madura, R. W. Impey, and M. L. Klein, The Journal of chemical physics **79**, 926 (1983).

[28] W. L. Jorgensen, J. D. Madura, and C. J. Swenson, Journal of the American Chemical Society **106**, 6638 (1984).

[29] R. Bosque and J. Sales, Journal of chemical information and computer sciences **42**, 1154 (2002).

[30] K. Sheppard.

[31] H. Flyvbjerg and H. G. Petersen, J. Chem. Phys. **91**, 461 (1989).

[32] L.-P. Wang, T. J. Martínez, and V. S. Pande, The Journal of Physical Chemistry Letters (2014).

[33] C. J. Fennell, L. Li, and K. A. Dill, The Journal of Physical Chemistry B **116**, 6936 (2012).

[34] I. V. Leontyev and A. A. Stuchebrukhov, The Journal of chemical physics **141**, 014103 (2014).

[35] A. D'Aprano and I. D. Donato, Journal of Solution Chemistry **19**, 883 (1990).

[36] W. M. Haynes, *CRC handbook of chemistry and physics* (CRC Press, 2011).

[37] D. L. Mobley, *Experimental and calculated small molecule hydration free energies*, Retrieved from: https://github.com/choderalab/FreeSolv, uC Irvine: Department of Pharmaceutical Sciences, UCI.

[38] J.-F. Truchon, A. Nicholl's, J. A. Grant, R. I. Iftimie, B. Roux, and C. I. Bayly, Journal of computational chemistry **31**, 811 (2010).

[39] J.-F. Truchon, A. Nicholls, B. Roux, R. I. Iftimie, and C. I. Bayly, Journal of chemical theory and computation **5**, 1785 (2009).

[40] J.-F. Truchon, A. Nicholls, R. I. Iftimie, B. Roux, and C. I. Bayly, Journal of chemical theory and computation **4**, 1480 (2008).

[41] J. Ponder, C. Wu, P. Ren, V. Pande, J. Chodera, M. Schnieders, I. Haque, D. Mobley, D. Lambrecht, R. DiStasio Jr, et al., J. Phys. Chem. B **114**, 2549 (2010).

[42] P. Ren and J. W. Ponder, The Journal of Physical Chemistry B **108**, 13427 (2004).

[43] G. Lamoureux and B. Roux, The Journal of Chemical Physics **119**, 3025 (2003).

[44] V. M. Anisimov, G. Lamoureux, I. V. Vorobyov, N. Huang, B. Roux, and A. D. MacKerell, Journal of Chemical Theory and Computation **1**, 153 (2005).

[45] L.-P. Wang, T. L. Head-Gordon, J. W. Ponder, P. Ren, J. D. Chodera, P. K. Eastman, T. J. Martínez, and V. S. Pande, J. Phys. Chem. B **117**, 9956 (2013).

[46] M. Frenkel, R. D. Chirico, V. V. Diky, Q. Dong, S. Frenkel, P. R. Franchois, D. L. Embry, T. L. Teague, K. N. Marsh, and R. C. Wilhoit, Journal of Chemical & Engineering Data **48**, 2 (2003).

[47] R. D. Chirico, M. Frenkel, V. V. Diky, K. N. Marsh, and R. C. Wilhoit, Journal of Chemical & Engineering Data **48**, 1344 (2003).

[48] *Mettler toledo density meters*, [Online; accessed 15-Jan-2015], URL http://us.mt.com/us/en/home/products/Laboratory_Analytics_Browse/Density_Family_Browse_main/DE_Benchtop.tabs.models-and-specs.html.

[49] R. D. Chirico, M. Frenkel, J. W. Magee, V. Diky, C. D. Muzny, A. F. Kazakov, K. Kroenlein, I. Abdulagatov, G. R. Hardin, and W. E. Acree Jr, Journal of Chemical & Engineering Data **58**, 2699 (2013).